

NJC

Accepted Manuscript



This article can be cited before page numbers have been issued, to do this please use: B. Paul, S. K. Sharma, S. Adak, R. khatun, G. Singh, D. Das, V. Joshi, S. Bhandari, S. S. Dhar and R. Bal, *New J. Chem.*, 2019, DOI: 10.1039/C9NJ01085H.



This is an Accepted Manuscript, which has been through the Royal Society of Chemistry peer review process and has been accepted for publication.

Accepted Manuscripts are published online shortly after acceptance, before technical editing, formatting and proof reading. Using this free service, authors can make their results available to the community, in citable form, before we publish the edited article. We will replace this Accepted Manuscript with the edited and formatted Advance Article as soon as it is available.

You can find more information about Accepted Manuscripts in the [author guidelines](#).

Please note that technical editing may introduce minor changes to the text and/or graphics, which may alter content. The journal's standard [Terms & Conditions](#) and the ethical guidelines, outlined in our [author and reviewer resource centre](#), still apply. In no event shall the Royal Society of Chemistry be held responsible for any errors or omissions in this Accepted Manuscript or any consequences arising from the use of any information it contains.

ARTICLE

Low temperature catalytic oxidation of aniline to azoxybenzene over Ag/Fe₂O₃ nanoparticle catalyst using H₂O₂ as an oxidantBappi Paul,^a Sachin K. Sharma,^a Shubhadeep Adak,^a Rubina Khatun,^a Gurmeet Singh,^a Dipak Das,^a Vedant Joshi,^a Sahil Bhandari,^a Siddhartha Sankar Dhar^b and Rajaram Bal^{*a}Received 00th January 20xx,
Accepted 00th January 20xx

DOI: 10.1039/x0xx00000x

An in-situ modified hydrothermal synthesis of Ag/Fe₂O₃ nanoparticles (NPs) and studies of its catalytic activity as a simple, eco-friendly and recyclable catalyst for one-pot conversion of aniline to azoxybenzene was performed. The as-synthesized nanostructured material was characterised by powder X-ray diffraction (XRD), transmission electron microscopy (TEM), scanning electron microscopy (SEM), SEM-mapping, temperature-programmed reduction (H₂-TPR), X-ray photoelectron spectroscopy (XPS), N₂ adsorption-desorption isotherm (BET), Fourier transform infrared spectroscopy (FT-IR), inductively coupled plasma-atomic emission spectroscopy (ICP-AES), ultraviolet-visible spectroscopy (UV-Vis) and vibrating sample magnetometer spectroscopy (VSM). The most active and recyclable catalyst with 2–5 nm diameters of metallic Ag particles supported on 10–50 nm Fe₂O₃ nanoparticles was formed with a silver loading of 1.8 wt%. High turnover number of ~592 was achieved with 92% conversion of aniline and 94% selectivity towards the target product azoxybenzene under atmospheric condition. The effect of various reaction parameters correspond to reaction time, temperature and substrates to H₂O₂ molar ratio were screened and studied in detail. The results reveals that the role of synergistic effect between the surface Ag nanoparticles and Fe₂O₃ nano-spheres for high catalytic activity.

Introduction

Selective oxidation of anilines is an important step for conversion of amines into a valuable industrial intermediates in the field of pharmaceuticals, food additives, therapeutic medicine, polymer stabiliser and liquid crystal display devices.^{1–5} Azoxybenzene as one of the oxidised product of anilines, is used as a starting material for Wallach rearrangement provide an easy synthetic route to synthesis hydroxyazobenzene which is applicable in coloration of dye, lacquer and resin.^{6,7} Azoxybenzene compounds falls in the class of N-oxides of azo compounds which are produced as an intermediate in the oxidation of aniline via dehydration of N-phenylhydroxyl amine and nitrosobenzene. These reaction pathway are quite harsh and lead to various intermediates. Therefore, the challenge lies in manipulation of reaction condition to increase the formation of desired product in the center of all conceivable oxidized products with reasonable conversion of the substrate. It is well documented in the

literature that various attempts have been made using stoichiometric and catalytic routes for oxidative coupling of aniline by using different oxidising agents. Aromatic amines get oxidized in presence of stoichiometric oxidants such as, MnO₂,⁸ Pb(OAc)₄,⁹ peracetic acid,¹⁰ BaMnO₄,¹¹ Hg(OAc)₂¹² and also in presence of various types of molecular sieves.¹³ Corma et al. has studied the oxidative coupling of aniline by molecular oxygen to azobenzene with high selectivity over Au–TiO₂ nanocatalyst.¹⁴ Recently, Ag/WO₃ and CuCr₂O₄ were found to be an excellent catalyst for selective oxidation of aniline to azoxybenzene.^{15,16} Although Ag/WO₃ catalyst has its own advantages, however considering the loading of silver percentage, conversion, selectivity and recovery of the catalyst after reaction still provides us enough scope for development of new catalyst. Li *et al.* has reported Ag nanostructured catalyst for room temperature selective oxidation of aniline to azobenzene at room temperature by using strong potassium hydroxide (KOH) and dimethyl sulfoxide (DMSO) as solvent.¹⁷ Lima et al. has reported that niobium oxyhydroxide promotes the catalytic activity of δ-FeOOH to convert aniline into azoxybenzene in the presence of hydrogen peroxide.¹⁸ Das et al. has found that Titanium-Loaded on MCM-48 act as an efficient catalyst for oxidation of aniline to azoxybenzene in presence of hydrogen peroxide.¹⁹ Recently, Silva *et al.* has reported sub-15nm CeO₂ nanowires with increased oxygen defects and Ce³⁺ Sites for Selective oxidation of aniline at room temperature in presence of H₂O₂.²⁰ Among the numerous oxidising agents H₂O₂ and O₂

^a *Catalytic Conversion & Processes Division, CSIR-Indian Institute of Petroleum, Dehradun- 248005, Uttarakhand, India.

^b Department of Chemistry, National Institute of Technology Silchar, Silchar- 788010, Assam, India.

*Corresponding authors. Fax: +91 135 2660202; Tel: +91 135 2525917

^c *E-mail: raja@iip.res.indrress

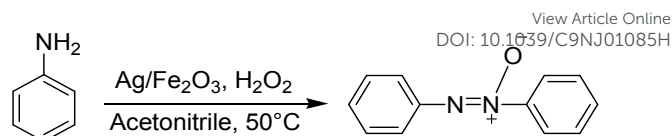
† Footnotes relating to the title and/or authors should appear here.

Electronic Supplementary Information (ESI) available: [details of any supplementary information available should be included here]. See DOI: 10.1039/x0xx00000x

ARTICLE

Journal Name

have their own significance and regarded as a greener oxidants. Although oxygen efficiency of molecular oxygen is greater than hydrogen peroxide, but still it requires drastic reaction condition to activate the oxygen at usual temperature and pressure in presence of heterogeneous catalytic system. Thus, from the safety and economical point of view, hydrogen peroxide is a better oxidant over molecular oxygen. But the reusability of the catalysts separation of the product from the reaction mixtures become two major challenges in liquid-phase organic transformation. Therefore, a recyclable catalyst that works under mild reaction condition is in high demand. Magnetic nanoparticles are highly desirable material as catalysts or catalyst supported materials in comparison with other transition metals oxides, iron oxide has been recognized as a green catalyst or support because of its low toxicity, mild reaction conditions, high thermal, mechanical stability and high catalytic activity.²¹⁻²³ Magnetic separation is a very efficient technique for the separation of magnetic particles from reaction mixture make them ideal catalyst for liquid phase organic reaction.²⁴ Among all the oxides of iron hematite ($\alpha\text{-Fe}_2\text{O}_3$) is one of the most desirable iron oxide nanomaterials due to their versatile applications as a catalyst in various reactions.²⁵⁻²⁶ Recently, nano-iron oxide catalyzed oxidation of alcohols and olefins has been studied using hydrogen peroxide as an oxidant.²⁷ Noble silver metal nanomaterials supported on iron oxide have shown tremendous potentials in various fields including catalysis. Several methods have been developed for the synthesis of silver supported nanoparticles. However synthesis of nanoparticles with desired shape, size and morphology is still considered a challenging proposition. Jiang *et al* had reported in situ synthesis of Ag nanoparticles on nanoporous Fe_2O_3 microboxes simply by annealing Prussian blue (PB) in the presence of silver nitrate.²⁸ Cui *et al* has successfully fabricated superhydrophobic Ag- Fe_2O_3 /Fe surfaces on iron substrates with a basic and simple replacement deposition method.²⁹ Kulkarni *et al* has synthesized Ag@ Fe_2O_3 nanoparticles by leaf extract assisted process where leaf of *Adathoda vasica* plant act as a capping agent as well as a reducing agent.³⁰ Recently, Paul *et al* has reported in situ synthesis of Ag/ Fe_2O_3 decorated on reduced graphene oxide nanocomposite via one-pot hydrothermal synthesis procedure, where polyethylene glycol act as surfactant to control the size and morphology of the nanomaterials.³¹ We report herein the preparation of highly dispersed ~2–5 nm silver nanoparticles supported on nanocrystalline iron oxide via cetyltrimethylammonium bromide assisted hydrothermal method followed by calcination for the selective oxidative coupling of aniline to azoxybenzene under very mild reaction condition (Scheme 1).



Scheme 1. Oxidative of aniline to azoxybenzene

Experimental

Synthesis of catalyst

Silver supported iron oxide nanoparticles was synthesized by adapting our own surfactant assisted hydrothermal method.²⁴ Adapting this synthesis procedure large quantity (up to 30 g) of catalyst can be synthesized with highly reproducibility. An amount of 24.539 g of ferric nitrate nonahydrate ($\text{Fe}(\text{NO}_3)_3 \cdot 9\text{H}_2\text{O}$) and 0.472 g of silver nitrate (AgNO_3) were dissolved distinctly in minimum volume of deionized water. The resultant clear solutions of silver nitrate were then mixed to the ferric nitrate solution and stirred magnetically. After stirring for 15 min 16.822 g of hexamine and 1.8 g cetyltrimethylammonium bromide (CTAB) was dissolved in water and ethanol mixture (50 ml water and 2 ml ethanol) and was added to the solution, followed by the addition of 0.4 g hydrazine. After stirring for 4 h, the reddish suspension was collected and the solution mixture was transferred into a stainless steel autoclave and heated at 180 °C for 24. The obtained solid material was centrifuged and washed with excess of H_2O and ethanol followed by drying for 12 h at 80 °C. The as-obtained precursor powder was then calcined in a muffle furnace for 4 h at 550°C to obtain powder of Ag/ $\alpha\text{-Fe}_2\text{O}_3$. ICP-AES analysis was performed to confirm the loading of the silver nanoparticles. The catalyst was also prepared by co-precipitation and impregnation methods.

Oxidative coupling of aniline

Catalytic oxidation of aniline was performed in a 50 ml round bottom flask with continuous stirring (800 rpm) in an oil bath. In a typical procedure, 0.1 g nanostructured catalyst, was dispersed in a 10 ml acetonitrile solution under sonication. Subsequently, 1 g of substrate (aniline) and 2.15 g H_2O_2 (50% aq. solution) was added drop wise under continuous stirring. At regular intervals small portion of the reaction mixture were withdrawn for analysis. The solid nanostructured catalyst was separated from the reaction mixture by an external magnet. The final products were examined using a gas chromatograph (Agilent 7890B). The Carbon balance was performed for the reaction and it was found to be between 98% \pm 2.

Results and discussion

Catalyst characterization

The powder XRD patterns of the synthesized Ag/ α -Fe₂O₃ nanoparticles was indexed with all the peaks at 2 θ values 24.1°, 33.3°, 35.6°, 40.8° and 49.6° confirming the formation of rhombohedrally structured α -Fe₂O₃ (JCPDS # 87-1166, space group: R3/c). (Fig. 1). The peaks patterns of α -Fe₂O₃ matches well with the reported peaks, with the highest intensity peak at a 2 θ value of 33.3°, which is referred to the plane (104). In addition to the diffraction peaks of α -Fe₂O₃ we could observed two additional intense peak at 2 θ values of 38.1 and 44.3° corresponds to (111) and (200) of Ag(0) which also match well with the literature reported values (JCPDS # 89-3722). No change in phase of Ag was observed for the reused catalyst indicating that the catalyst is active even after cycle of reuse. The loading of silver present in the Ag/ α -Fe₂O₃ nanocrystalline material was confirmed by ICP-AES.

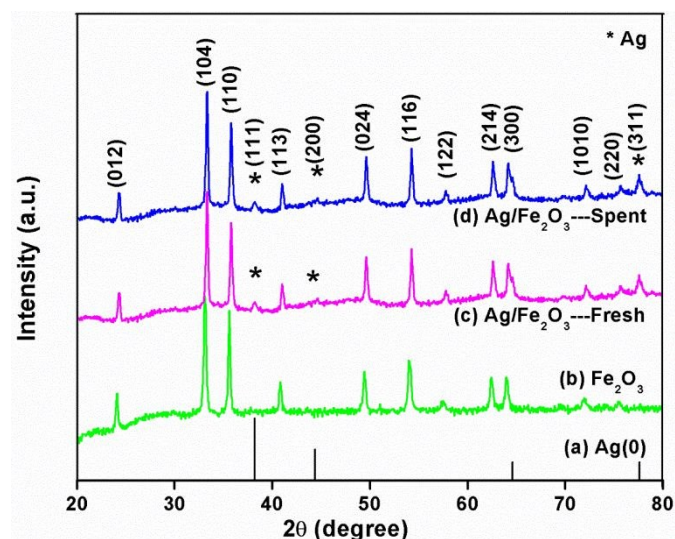


Figure 1. Powder XRD patterns of Ag/ α -Fe₂O₃ nanoparticles.

The morphology and the structural properties of the synthesized Ag/ α -Fe₂O₃ nanoparticles was determined by SEM analysis. The representative SEM images of the catalyst shows almost spherical shape of size 20-50 nm (Fig. 2(a,b,c)). The EDS spectra of the synthesized nanoparticles exhibited only the presence of iron, silver and oxygen and no other peaks of impurities could be identified in the spectra (Fig. 2d).

In order to confirm the dispersion of silver on the nanocrystalline α -Fe₂O₃ elemental mapping of the as synthesized material was performed. The results reveals the homogenous distribution of Ag on nanocrystalline α -Fe₂O₃ support (Fig. 3). It could be observed from the mapping that silver nanoparticles are distributed throughout the support, which confirms the uniform loading of silver.

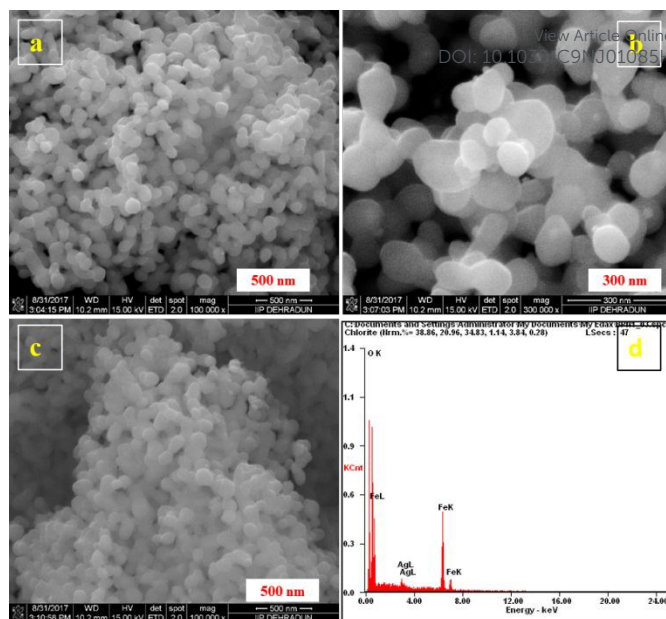


Figure 2. SEM images of the (a, b) fresh and (c) spent catalyst and (d) the SEM-EDS mapping of the fresh catalyst.



Figure 3. Elemental mapping of Ag/ α -Fe₂O₃ (a) Fe, (b) O, and (c) Ag.

The particle size and distribution of the silver over Fe₂O₃ nanoparticles was carried out using high resolution transmission electron microscopy (HRTEM) analysis (Fig. 4). TEM image reveals almost spherical shape Fe₂O₃ nanoparticles with size 20-50 nm. It was also observed from the TEM analysis that small spherical size silver nanoparticles distributed throughout the spherical shape Fe₂O₃ nanoparticles with an average size of Ag particles within the range of 2–5 nm. Moreover, from the HRTEM image we could observed the lattice fringes separated by 0.25 nm and 0.23 nm, corresponds to (110) and (111) plane for Fe₂O₃ and Ag(0) respectively. Moreover, the HRTEM image of the reused catalyst (Fig. S1 in ESI) shows almost same shape and size even after cycle of recyclability test. The corresponding particle size distribution histogram of Ag particles with sizes between 2 and 5 nm indicates a very narrow particle size distribution which is in good agreement with the PXRD (Fig. 4a, inset).

The metal-support interactions (Ag-Fe) and the reduction behaviour within the catalysts were compared by H₂-temperature-programmed-reduction (TPR) (Fig. 5). The synthesized nanomaterial exhibited two broad reduction peaks at high temperature, the peak around 350 °C can be attributed to the reduction of Fe₂O₃ to Fe₃O₄ and the other wide peaks at higher temperatures around 500°C can be documented due to transformation of Fe₃O₄ → FeO → Fe-metal.

ARTICLE

It was also observed from the TPR profile that with the loading of silver on the support (Fe_2O_3), both the reduction peak (around 400 and 800) shifted to lower temperatures compared to the support. The study confirmed that loading of Ag enhanced the reduction of Fe_2O_3 which further leads to strong metal support interaction between the active metal (Ag) and the support ($\alpha\text{-Fe}_2\text{O}_3$). This perhaps takes place through the spill over of hydrogen from the silver atoms to iron oxide.^{32,33}

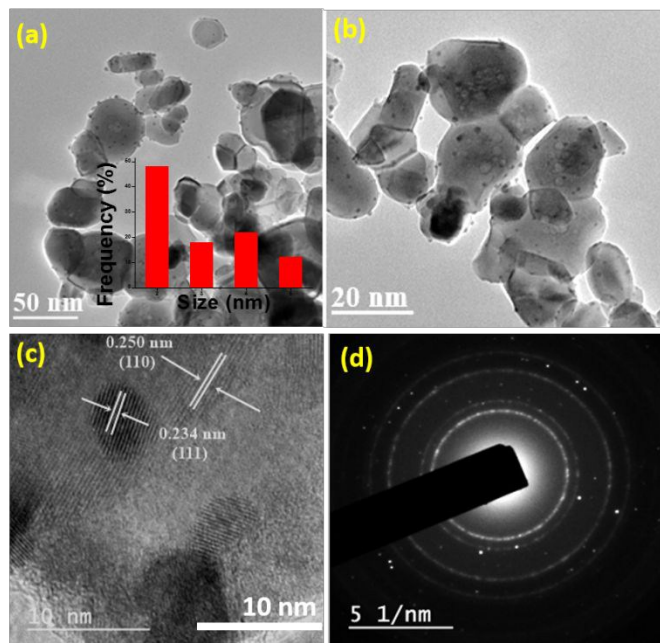


Figure 4. (a, b) TEM images (inset Ag particle size distribution), (c) HRTEM image (lattice fringes) and (d) ED pattern of $\text{Ag}/\alpha\text{-Fe}_2\text{O}_3$ nanoparticles

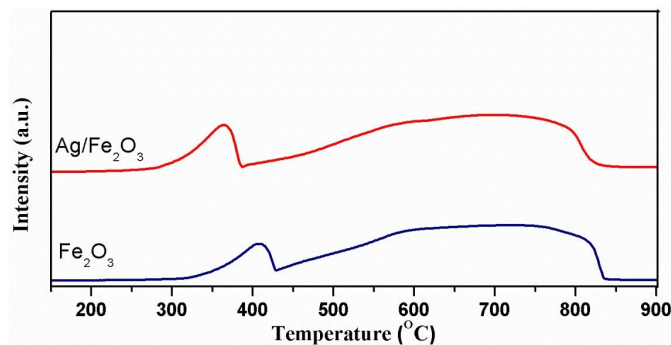


Figure 5. TPR profile of (a) Fe_2O_3 (b) $\text{Ag}/\text{Fe}_2\text{O}_3$ nanoparticles.

To confirm the valence state of Ag nanoparticles in $\text{Ag}/\alpha\text{-Fe}_2\text{O}_3$ nanostructured catalyst X-ray photoelectron spectroscopy (XPS) was performed where the presence of metallic silver could be clearly identified which corresponds to $3d_{5/2}$ and $3d_{3/2}$ with binding energy around 368.3 eV and 374.2 eV respectively (Fig. 6a). The $\text{Fe } 2p_{3/2}$ and $2p_{1/2}$ spectra attributed to the binding energies 710.6 eV and 724.2 eV respectively suggest that the binding energies of Fe^{3+} in Fe_2O_3 . (Fig. 6(b)). In addition to that a satellite peak at 717.6 eV is characteristic of Fe^{3+} ions in $\alpha\text{-Fe}_2\text{O}_3$.³³ After deconvolution of oxygen ($\text{O } 1s$)

spectrums we could observed three different peaks at the binding energies of 533.2, 531.8 and 529.8 eV corresponds to the adsorbed oxygen (O_{ads}), hydroxyl oxygen (O_{hyd}) and lattice oxygen (O_{latt}), respectively.^{33,34} Whereas the XPS analysis of the spent catalyst confirms that the intact of oxidation state of silver (Ag^0) during the catalysis (Figure S2 in ESI).

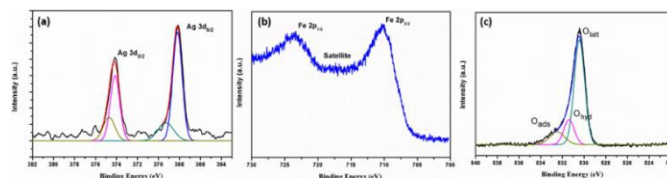


Figure 6. (a) $\text{Ag } 3d_{3/2}$ spectrum (b) $\text{Fe } 2p$ spectrum (c) $\text{O } 1s$ spectrum of the $\text{Ag}/\alpha\text{-Fe}_2\text{O}_3$ catalyst.

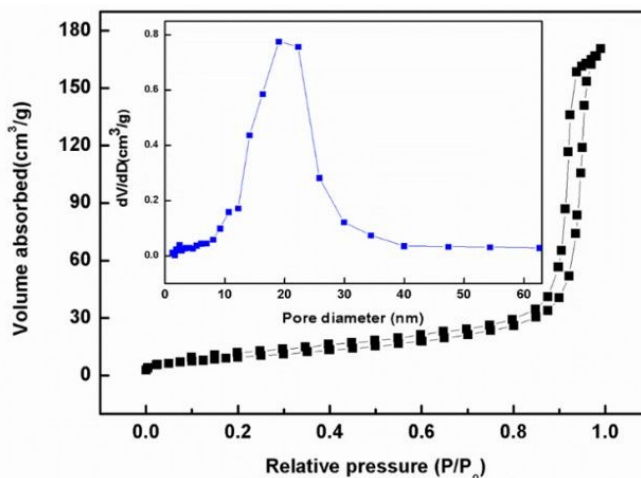


Figure 7. N_2 adsorption-desorption isotherm and pore size distribution curve (inset) of $\text{Ag}/\alpha\text{-Fe}_2\text{O}_3$ nanoparticles.

To analysis the surface area of the synthesized nanoparticles ($\text{Ag}/\alpha\text{-Fe}_2\text{O}_3$) N_2 physisorption measurements (BET) was conducted. The N_2 adsorption-desorption isotherms of the synthesized nanostructured material exhibits high specific surface area and pore volume. The amount of N_2 adsorbed rise gradually at lower relative pressures and then increased sharply at higher relative pressures (Fig.7). The sample exhibits type-IV adsorption-desorption isotherm with a type H_2 hysteresis loop in the P/P_0 range from 0.80 to 0.95. The pores are predominantly in the range from 3 to 15 nm as confirmed by pore size distribution which is justified from the TEM images (inset of Fig.7).

The surface-coordinating organic template (CTAB) on the uncalcined catalyst ($\text{Ag}/\text{Fe}(\text{OH})_3$ precursor) was analysed by FTIR spectroscopy (Fig. S3 in ESI). To study the nature of interaction and occurrence of the template molecules with the Fe-O surface, FTIR-spectrum of clean CTAB with that of uncalcined $\text{Ag}/\text{Fe}(\text{OH})_3$ precursor were studied. For pure CTAB, the stretching vibrations of the ammonium group appeared at 1487 and 1472 cm^{-1} ($\nu_{\text{asym}}(\text{CH}_3\text{-N}^+)$) and 1439 cm^{-1} ($\nu_{\text{sym}}(\text{CH}_3\text{-N}^+)$). The characteristic absorption bands for CTAB in the Ag-Fe sample appeared at 1640 cm^{-1} ($\nu_{\text{asym}}(\text{CH}_3\text{-N}^+)$) and 1410 cm^{-1}

($v_{\text{sym}}(\text{CH}_3\text{-N}^+)$). It can be incidental that mutual interactions between template and the surface of Ag-Fe have taken place. The peaks at 809 and 1062 cm^{-1} corresponds to the C-N⁺ stretching vibration of CTAB molecules. The frequencies beyond 1600 cm^{-1} to 3000 cm^{-1} can be attributed to the CH₂ symmetric and antisymmetric stretching vibrations respectively. The band at 609 and 471 cm^{-1} are attributed to Fe-O bond in tetrahedral and octahedral site in Fe₂O₃. After the calcination of nanostructured material we could observe the absence of all the typical frequencies of the surfactant (CTAB) which confirm that the removal of surfactant moieties from the materials. However, we could observe the absorption bands at 608 and 517 cm^{-1} even after calcination which refers to the typical peak of Fe-O (metal oxide). Furthermore, no peaks of C, N or Br were detected from the SEM-EDS diagram of catalyst which confirms the removal of the template (CTAB) after calcination. The surface-coordinating organic surfactant CTAB molecules on the pre-calcined catalyst surface were further confirmed from the TGA. Two step decomposition pathways were observed from the TGA curve (Fig.S4 in ESI). In the first step (30-100°C) the weight loss of 8.04% was observed due to the decomposition of physically adsorbed moisture. In the second step the weight loss of 73.33 % around 280-520°C was observed, indicating the removal of CTAB from the nanoparticles surface and conversion of Ag/Fe(OH)₃ to Ag/ α -Fe₂O₃ nanoparticles. TGA curve of the catalysts after calcination does not show the presence of any organic impurities which conforms the complete removal of the surfactant CTAB (Fig. S5 in ESI). The UV-Vis DRS absorption spectrum of Ag/ α -Fe₂O₃ (after calcination) is shown in Fig. S6 in ESI. The absorption peak shows bands around 475 nm and 550 nm which are due to the presence metallic silver nanoparticles and hematite nanostructures, which confirm the presence of metallic silver nanoparticles supported over iron oxide nanostructures. The physicochemical properties of the fresh and spent catalyst is summarised in Table 1.

Table 1. Physicochemical Properties of the Ag/ α -Fe₂O₃ Nanoparticles Catalyst

Catalyst	Ag loading ^a (%)	BET Surface area (m ² /g)	Morphology	Average particles size		
				From XRD ^b		From TEM
				Fe ₂ O ₃	Fe ₂ O ₃	Ag
Ag/Fe ₂ O ₃	1.8	35.4	Uniform dispersed Spherical	33.7	32	3.8
Ag/Fe ₂ O ₃ (Spent, after 5 cycle)	1.6	35.9	Uniform dispersed Spherical	33.1	32	3.6

^aEstimated by ICP-AES. ^bMeasured using Scherrer equation.

The room temperature magnetic hysteresis studies of Ag/ α -Fe₂O₃, with the magnetic field applied extensive from -20000 G to +20000 G (Fig.S7 in ESI). The VSM hysteresis loops exhibited

a ferromagnetic behaviour with a saturation magnetization of around 33.4, coercivity (H_c) of 310.06 G and remnant magnetization (M_r) of 8.42 emu g⁻¹.

Catalytic activity

After the fruitful synthesis and characterization of nanostructured catalyst (Ag/ α -Fe₂O₃), we extend our studies to evaluate its catalytic efficiency for oxidative coupling reaction of various aromatic substituted amines where aniline was selected as a standard substrate and various reaction parameter was evaluated such as temperature, time, catalyst amount and aniline: H₂O₂ molar ratio in order to get finest selectivity and yield of azoxybenzene. When the catalytic performance were evaluated by using H₂O₂ as oxidant and acetonitrile (CH₃CN) as a solvent with aniline: H₂O₂ mole ratio (1 : 3) for 8 h at 50 °C, the catalyst exhibited 94% selectivity towards azoxybenzene with maximum aniline conversion of 92% were nitrobenzene, nitrosobenzene and azobenzene were spotted as the by-products of the reaction. When the molar ration of aniline and H₂O₂ was 1 : 1, we observed 40% conversion of aniline with 60% azoxybenzene selectivity (very low), which is believed due to the lesser interaction between active oxidising species and the reactant. When the aniline to H₂O₂ mole ratio is increased up to five times (1:5), the conversion of aniline is increased up to 97% and the selectivity of azoxybenzene decreased to 72% with the increase in selectivity for nitrobenzene, which may be due to over oxidation in the presence of excessive active oxygenated species (Fig. 8).

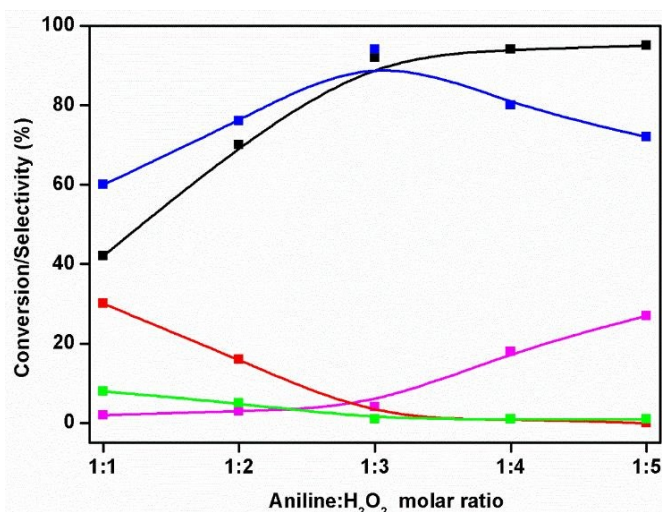


Figure 8. Effect of the aniline: H₂O₂ molar ratio on catalytic oxidation of aniline [■] aniline conversion, [■] azoxybenzene selectivity, [■] nitrobenzene selectivity, [■] azobenzene selectivity, [■] nitrosoaniline selectivity. Reaction Condition solvent = CH₃CN; catalyst weight = 0.10 g; substrate= aniline (1 g); time = 8 h; temperature 50°C.

When the temperature is low, the selectivity of azoxybenzene was found to be 90% with 42 % conversion of aniline, with the increase of temperature up to 70 °C, the conversion increases

progressively but the selectivity decreases as the increase in formation of nitrobenzene as the side product which may be due to the over oxidation of aniline or decomposition of H_2O_2 takes place at high temperature (Fig. 9). The effect of reaction time was also studied and it was observed that with the increase in time both the azoxybenzene selectivity and aniline conversion increases (Fig. 10). A sharp increase in the selectivity of azoxybenzene and conversion of aniline and with the decrease in the selectivity of nitroso benzene was observed after 4 h of reaction. Figure 10 shows the maximum selectivity towards azoxybenzene ($\sim 94\%$) was achieved at 8 h of reaction, but after 10 h the selectivity of azoxybenzene decreases to $\sim 78\%$ due to the formation of nitrobenzene. The individual role of Ag and Fe_2O_3 was explored for the catalytic activity, where we have conducted a series of experiments.

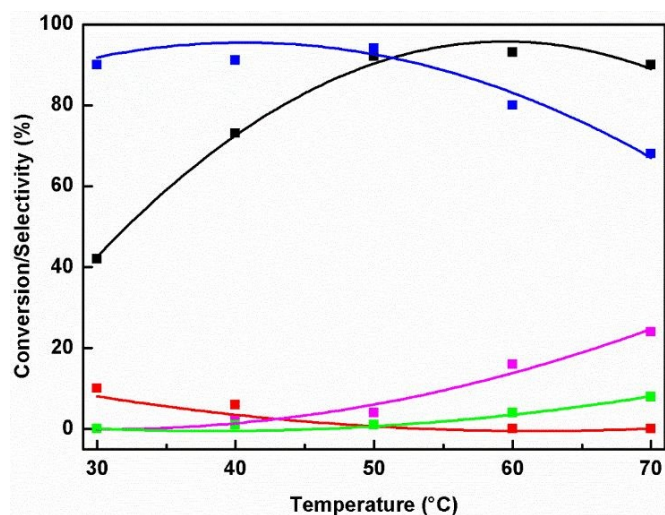


Figure 9. Effect of temperature ($^{\circ}\text{C}$) on catalytic oxidation of aniline. ■ aniline Conversion, [■] azoxybenzene selectivity, [■] nitrobenzene selectivity, [■] azobenzene selectivity, [■] nitrosoaniline selectivity. Reaction Condition solvent = CH_3CN ; catalyst weight = 0.10 g; substrate= aniline(1 g); substrate : H_2O_2 mole ratio = 1 : 3; time = 8 h.

Negligible amount of aniline conversion was observed in absence of the catalyst (Table 2, entry 10). When the catalytic activity of $\text{Ag}/\alpha\text{-Fe}_2\text{O}_3$ synthesized by our present preparation method was studied it was observed that the catalyst showed excellent conversion of aniline (Table 2, entry 6). When the Ag loaded on $\alpha\text{-Fe}_2\text{O}_3$ by impregnation method (imp), it exhibit poor activity behaviour due to increase in sizes of particle and the leaching of active metals (Table 2, entry 5). Furthermore, the $\text{Ag}/\alpha\text{-Fe}_2\text{O}_3$ nanostructured catalyst synthesized by our preparation method showed high TON of 592.0 for the formation of azoxybenzene with greater H_2O_2 efficiency of $\sim 27.1\%$, compared to simple Ag or Fe_2O_3 catalyst (Table 2, entries 3 and 4). It is believed that excellent catalytic activity shown by the present catalyst ($\text{Ag}/\alpha\text{-Fe}_2\text{O}_3$) synthesized by our present method is due to high specific surface area ($35.4\text{ m}^2/\text{g}$) and excellent dispersion of small sized Ag nanoparticles supported on Fe_2O_3 which leads to easy accessibility active catalytic sites of the catalyst and the reactants. Thus, from the

results of the optimization studied of the reaction parameter and $\text{Ag}/\alpha\text{-Fe}_2\text{O}_3$ as a standard catalyst, various other substituted aniline reactions were performed. Table 3 summarized the results of various other substituted aniline. Various substituted anilines bearing electron withdrawing and electron donating groups were examined and was found to be selectively transformed to their corresponding substituted azoxy products with high to excellent yield.

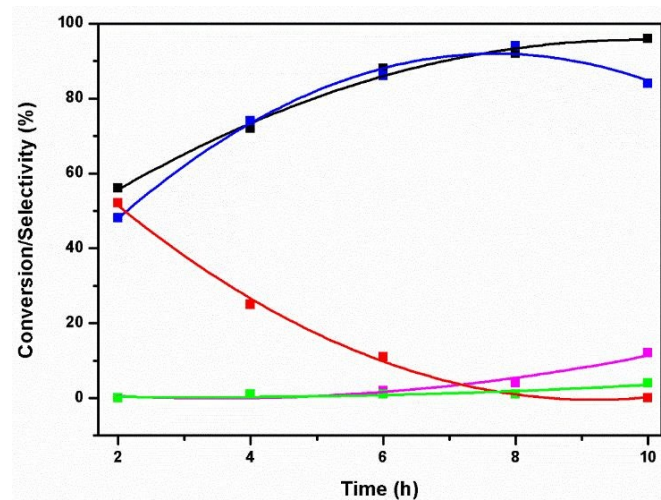


Figure 10. Effect of time on catalytic oxidation of aniline. ■ aniline conversion of [■] azoxybenzene selectivity, [■] nitrobenzene selectivity, [■] azobenzene selectivity, [■] nitrosoaniline selectivity. Reaction condition solvent = CH_3CN ; catalyst weight = 0.10 g; substrate= aniline (1 g); substrate : H_2O_2 mole ratio = 1 : 3; temperature 50°C .

The oxidative coupling of aniline to azoxybenzene over $\text{Ag}/\alpha\text{-Fe}_2\text{O}_3$ nanostructured catalyst is assumed to follow the radical pathway as illustrated in Scheme S1 in ESI. According to the previous reported literature, in the first step H_2O_2 decompose over Ag NPs to form superoxide ($\text{O}_2^{\cdot-}$) conferring to the reaction mechanism shown in eqn (i). In the second step the generated superoxide ($\text{O}_2^{\cdot-}$) from Ag(0) yields peroxide species $\bullet\text{OOH}$, which acts as the active species for this catalytic reaction eqn (ii).³⁵⁻³⁸ Subsequently, the adsorption of aniline onto the surface of iron oxide take place through electrostatic interactions. This active peroxide species ($\bullet\text{OOH}$) then combine with the N-H bond of aniline, which is slightly electropositive in nature by donating its lone pair of electron to iron. Nitrosobenzene and phenyl hydroxyl amine were found to be a main intermediates for this reaction, which consensuses well with the literature report for the oxidation of aniline in presence of H_2O_2 .^{15,16} It is assumed that the reaction take place step by step, where at the preliminary aniline get oxidizes to phenyl hydroxyl amine, which further oxidizes to azobenzene. Finally azobenzene oxidizes to form azoxybenzene.

Table 2. Oxidative coupling of aniline to azoxybenzene^aView Article Online
DOI: 10.1039/C9NJ01085H

Entry	Catalyst	C _T ^b (%)	Selectivity S _p ^c (%)				Yield Y _A ^d (%)	Turnover number (TON)	H ₂ O ₂ efficiency (%)
			Nitro benzene ^e	Nitroso benzene	Azo benzene ^e	Azoxy benzene			
1	Ag ^{com}	3.6	11	41	48	-	-	-	
2	Fe ₂ O ₃ ^{com}	11	8	47	6	2.4	-	-	
3	Ag ^{us}	32	13	31	52	1.3	205.9	0.4	
4	Fe ₂ O ₃ ^{us}	27	17	36	2	12.2	173.7	3.8	
5	Ag/Fe ₂ O ₃ ^{imp}	18	38	3	7	9.4	115.8	2.9	
6	Ag/Fe ₂ O ₃ nano catalyst ^e	92	4	1	1	94	86.5	592	27.1
7	Ag/Fe ₂ O ₃ nano catalyst ^f	91	7	1	1	92	83.72	585.6	26.2
8	Ag/Fe ₂ O ₃ nano catalyst ^g	99	-	-	4	96	95.0	543.7	35
9	Ag/Fe ₂ O ₃ nano catalyst ^h	99	-	-	-	99	98.0	325.6	60.3
10	No Catalyst	1	-	-	-	-	-	-	

^a Reaction conditions: CH₃CN = 10 ml, aniline = 1 g, catalyst = 0.10 g with silver loading = 1.8 wt%, temperature = 50°C; time = 8 h; aniline : H₂O₂ mole ratio = 1 : 3; ^b C_T: aniline conversion analysed by GC = [aniline reacted in mols/aniline used in mols] × 100. ^c S_p: moles of the product / moles of aniline converted; ^d Y_A Yield = conversion × selectivity/100; ^e ~Silver nanoparticles supported on Fe₂O₃. ^f Catalyst after 5 cycle of reuse; ^g When reactant phenyl hydroxyl amine was used, time = 6 h; ^h When reactant azobenzene was used, time = 4 h; imp = impregnation method; com = commercial; us = bare Ag and Fe₂O₃ synthesized by our method. H₂O₂ efficiency = [moles of azoxybenzene formed/total moles of H₂O₂ added] × 100.

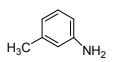
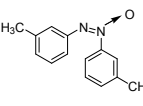
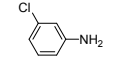
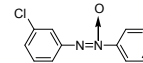
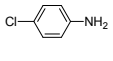
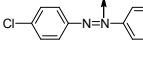
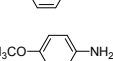
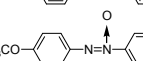
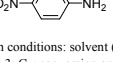
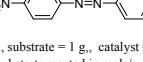
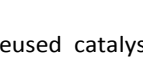
In order to get more idea about the reaction pathway and the formation of intermediate, a reaction was carried out separately with all the intermediates under the same reaction condition in presence of Ag/α-Fe₂O₃ as catalyst. Where phenyl hydroxyl amine and azobenzene produced azoxybenzene within 6 h and 4 h of reaction time respectively (Table 2, entry 9) which confirm the presence of phenyl hydroxyl amine as well as azobenzene as intermediates in the reaction for the formation of azoxybenzene.

In order to confirm the radical formation in the reaction mixture, p-benzoquinone was added in the reaction mixture where we observed aniline conversion up to 84% with 95% selectivity towards azoxy benzene within 6 h of reaction time. On the other hand, equimolar quantity of 2,6-di-tert-butyl-4-(4-methoxyphenyl)phenoxy (DBMP) was added to the reaction mixture as a radical scavenger to confirm the radical formation. The reaction was virtually suppressed under this reaction condition with aniline conversion of ~14% even after 24 h of continuous reaction. From all these above observation it propose, the increasing in the reaction rate with the addition of p-benzoquinone, whereas 2,6-di-tert-butyl-4-(4-methoxyphenyl)phenoxy retards it. Which confirm a radical pathway for our present catalytic system.

After the reaction was completed, the nanostructured solid catalyst was magnetically recovered from the reaction mixture followed by washing with ethanol and reused for numerous

catalytic cycles to check the adeptness and efficiency of the catalyst. The nanostructured catalyst remain active even after 5 consecutive cycle without decline in the catalytic activity which confirms true heterogeneity of the catalyst (Fig.11(a)).

Table 3. Oxidative coupling of of different substituted anilines^a

Entries	Substrate	C _T (%)	Product	Selectivity (%)	Yield (%)	TON
1		74		84	62.1	413.8
2		90		94	84.6	422.8
3		90		92	82.8	422.8
4		89		90	80.1	480.0
5		90		86	77.4	437.9
6		72		68	49.0	312.6

^a Reaction conditions: solvent (CH₃CN) = 10 ml, substrate = 1 g., catalyst = 0.10 g, time = 8 h; substrate: H₂O₂ molar ratio = 1 : 3; C_T: conversion analysed by GC = [substrate reacted in mols/substrate used in mols] × 100; Selectivity total moles of the product formed/total moles of substrate converted; Yield = conversion × selectivity/100

The TEM image of the reused catalyst exhibited an almost similar shape and size to that of the fresh synthesized catalyst (Fig S1 in ESI). The heterogeneity of the catalyst was further

confirmed from the ICP-AES analysis where the amount of Ag and Fe remain nearly same even after five consecutive cycle with negligible amount of silver leaching (concentration of both metals were <2 ppb). Conventional hot filtration test was performed to confirm no leaching of silver particles from the support during the reaction, where the catalyst was removed after 4 hour of the catalytic reaction.³⁹ After 4 hour of catalytic reaction the yield of the product was noted. The catalyst was separated and the reaction mixture and was further continued for another 6 hours, no noticeable increase in the yield of the product was observed. Which confirms the absence of leaching of Ag particles from the support (Fe₂O₃) in the course of reaction (Fig.11(b)).

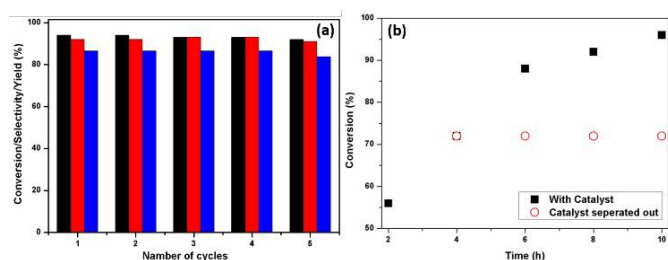


Figure 11. (a) Recyclability test of Ag/Fe₂O₃ nanostructured catalyst. [■] Aniline conversion of, [■] azoxybenzene selectivity, [■] azoxybenzene yield. (b) Sheldon's hot filtration test. Reaction Condition solvent = CH₃CN; aniline = 1 g; catalyst weight = 0.10 g; substrate: H₂O₂ molar ratio = 1: 3; time = 8 h; temperature 50°C.

It was also confirmed from the XPS analysis, that the oxidation state of silver remain intact during the catalytic reaction (Fig S2 in ESI). In Table S1 in ESI, we try to make comparison of the most relevant catalytic system with our catalyst in regard to selective oxidative coupling of aniline to azoxybenzene. From the comparison table and the summary of activity data of aniline oxidation, it is signify that our Ag/Fe₂O₃ catalyst with 1.8 wt.% Ag-loading shows good catalytic activity at 50 °C compare to other literature report. Our present catalyst Ag/Fe₂O₃ is expected to find a reasonable place in the literature on oxidation of aniline to azoxybenzene.

Conclusions

We have described herein a facile and simple surfactant assisted hydrothermal preparation of Ag NPs supported Fe₂O₃ nanoparticles catalyst. The synthesized material were characterized by powder XRD, BET surface area, SEM, HRTEM, ICP-AES, TGA, FT-IR, UV-Visible, and XPS analysis. HRTEM studies showed the presence of homogeneously distributed Ag-nanoparticles with size 2–5 nm supported on Fe₂O₃ nanoparticles with size 10–50 nm. The H₂-TPR studies also indicate that the highly dispersed Ag particles are strongly interacted with Fe₂O₃ support. The catalyst with 1.8% Ag loading was found to be the optimum loading for the selective oxidative coupling of aniline with 92% aniline conversion and

94% azoxybenzene selectivity at 50 °C with H₂O₂ as oxidant. In this present studies the synthesized nanostructured catalyst showed true heterogeneity as its effectiveness remains unchanged even after five consecutive cycles.

Conflicts of interest

There are no conflicts to interest.

Acknowledgements

B.P thanks SERB-DST, New Delhi, for financial support in the form of National Post-Doctoral fellowship (PDF/2016/001948). Director IIP, is acknowledged for his encouragement and support.

References

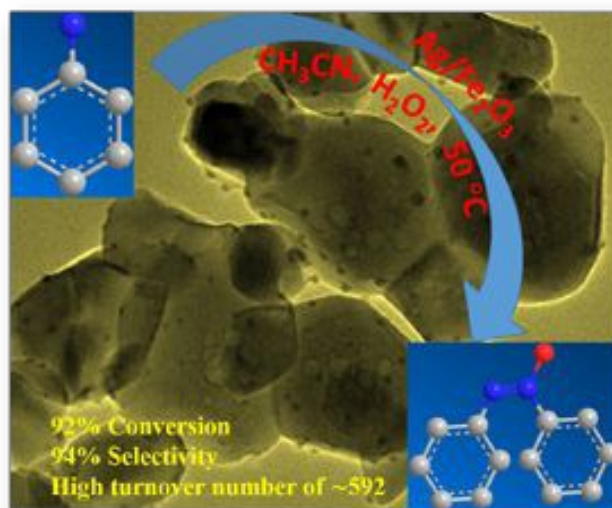
1. S. C. Catino and E. Farris, Concise encyclopedia of chemical technology; John Wiley & Sons: New York, 1985, Chapter 7.
2. S. Sakuae, T. Tsubakino, Y. Nishiyama and Y. Ishii, *J. Org. Chem.*, 1993, **58**, 3633-3638.
3. S. Chen, G. Lu and C. Cai, *New J. Chem.*, 2015, **39**, 5360-5365
4. E. R. Burkhardt and K. Matos, *Chem. Rev.*, 2006, **106**, 2617-2650.
5. A. M. Tafesh and J. Weiguny, *Chem. Rev.*, 1996, **96**, 2035-2052.
6. E. Buncel, *Can. J. Chem.*, 2000, **78**, 1251-1271.
7. E. Buncel, *Acc. Chem. Res.*, 1975, **8**, 132-139.
8. O. H. Wheeler and D. Gonzalez, *Tetrahedron*, 1964, **20**, 189-193.
9. H. E. Baumgarten, A. Staklis and E. M. Miller, *J. Org. Chem.*, 1965, **30**, 1203-1206.
10. R.W. White and W.D. Emmons, *Tetrahedron*, 1962, **17**, 31-34.
11. H. Firouzabadi and Z. Mostafavipoor, *Bull. Chem. Soc. Jpn.*, 1983, **56**, 914-917
12. E. Wenkert and B. Wickberg, *J. Am. Chem. Soc.*, 1962, **84**, 4914-4919.
13. S.B. Waghmode, S. M. Sabne and S. Sivasankar, *Green Chem.*, 2001, **3**, 285-288.
14. A. Gorrane, A. Corma and H. Garcia, *Science*, 2008, **322**, 1661-1664.
15. S. Ghosh, S. S. Acharyya, T. Sasaki and R. Bal, *Green Chem.*, 2015, **17**, 1867-1876.
16. S. S. Acharyya, S. Ghosh and R. Bal, *ACS Sustainable Chem. Eng.*, 2014, **2**, 584-589.
17. S. Cai, H. Rong, X. Yu, X. Liu, D. Wang, W. He and Y. Li, *ACS Catal.*, 2013, **3**, 478-486.
18. A.L.D. Lima, D.C. Batalha, H.V. Fajardo, J.L. Rodrigues, M.C. Pereirab and A.C. Silva, *Catal. Today*, 2018, doi: 10.1016/j.cattod.2018.10.035
19. D.R. Das and A.K. Talukdar, *ChemistrySelect*, 2017, **2**, 8983-8989.
20. A.G.M. da Silva, D.C. Batalha, T.S. Rodrigues, E.G. Candido, S.C. Luz, I.C. de Freitas, F.C. Fonseca, D.C. de Oliveira, J.G. Taylor, S.I.C. de Torresi, P.H.C. Camargo and H.V. Fajardo, *Catal. Sci. Technol.*, 2018, **8**, 1828-839.
21. S. Kulkarni, M. Jadhav, P. Raikar, D.A. Barretto, S.K. Vootla and U.S. Raikar, *New J. Chem.*, 2017, **41**, 9513-9520
22. T. Chang, D. Zhang, H. Li and G. Liu, *Green. Chem.*, 2014, **16**, 3401-3427.
23. C. Plisson, A.D. Nowicki, C. Meriadec, J.M. Greneche and A.

- 1
2
3 Roucoux, *ChemCatChem*, 2015, **7**, 309-315
4 24. B. Paul, B. Bhuyan, D.D. Purkayastha and S.S. Dhar, *Catal.*
5 *Commun.*, 2015, **69**, 48-54.
6 25. H. Hong, L. Hu, M. Li, J. Zheng, X. Sun, X. Lu, X. Cao, J. Lu and
7 Gu. H. *Chem. Eur. J.*, 2011, **17**, 8726-8730.
8 26. X.L. Hu, J.C. Yu, J.M. Gong, Q. Li and G.S. Li, *Adv. Mater.*,
9 2007, **19**, 2324-2329.
10 27. F. Shi, M.K. Tse, M.M. Pohl, A. Bruckner, S. Zhang and M.
11 Beller, *Angew. Chem. Int. Ed.*, 2007, **46**, 8866-8868.
12 28. Z. Jiang, D. Jiang, A.M.S. Hossain, K. Qian and J. Xie, *Phys.*
13 *Chem. Chem. Phys.*, 2015, **17**, 2550-2559.
14 29. S. Cui, S. Lu, W. Xu, B. Wu, N. Zhao, G. He, X. Hou, and H.
15 Zhang, *New J. Chem.*, 2016, **40**, 8897-8904.
16 30. S. Kulkarni, M. Jadhav, P. Raikar, D.A. Barretto, S.K. Vootla
17 and U.S. Raikar, *New J. Chem.*, 2017, **41**, 9513-9520.
18 31. B. Paul, D.Dhar Purkayastha, S.S. Dhar, S. Das, S. Haldar, *J.*
19 *Alloys Compd.*, 2016, **681**, 316-323.
20 32. A.B. Ravandi, M. Rezaei and Z. Fattah, *Chem. Eng. J.*, 2013,
21 **219**, 124-130
22 33. K. Narasimharao, A.A. Shehri and S.A. Thabaiti, *Appl. Catal.*,
23 *A* 2015, **505**, 431-440.
24 34. X. Yang, H. Sun, L. Zhang, L. Zhao, J. Lian and Q. Jiang, *Sci.*
25 *Rep.*, 2016, **6**, 31591-31602.
26 35. E. Saion, E. Gharibshahi and K. Naghavi, *Int. J. Mol. Sci.*, 2013,
27 **14**, 7880-7896.
28 36. Y. Ono, T. Matsumura, N. Kitajima and S.-I. Fukurumi, *J. Phys.*
29 *Chem.*, 1977, **81**, 1307-1311.
30 37. J. Z. Guo, H. Cui, W. Zhou and W. Wang, *J. Photochem.*
31 *Photobiol., A*, 2008, **193**, 89-96.
32 38. A. M. Jones, S. Garg, D. He, A. N. Pham and T. D. Waite,
33 *Environ. Sci. Technol.*, 2011, **45**, 1428-1434.
34 39. H. E. B. Lempers and R. A. Sheldon, *J. Catal.*, 1998, **175**, 62-
35 69.

View Article Online
DOI: 10.1039/C9NJ01085H

ARTICLE

Graphical Abstract



Highly dispersed Ag supported α - Fe_2O_3 found to be recyclable and efficient catalyst for one-pot conversion of aniline to azoxybenzene